Adsorption of Polyelectrolyte Multilayers on Polymer Surfaces

A. Delcorte* and P. Bertrand

Department of Material and Processing Science, Unité de Physico-Chimie et de Physique des Matériaux, Université Catholique de Louvain, 1 Place Croix du Sud, B-1348 Louvain-la-Neuve, Belgium

E. Wischerhoff and A. Laschewsky

Department of Chemistry, Laboratoire de Cinétique et Macromolécules, Université Catholique de Louvain, 1 Place Louis Pasteur, B-1348 Louvain-la-Neuve, Belgium

Received February 3, 1997. In Final Form: June 3, 1997[⊗]

Different from the conventional use of charged supports, the assembly of thin coatings by alternate adsorption of oppositely charged polyelectrolytes was realized on a variety of uncharged standard polymers, such as poly(propylene), poly(styrene), poly(methyl methacrylate), and poly(ethylene terephthalate). For the multilayer buildup, the polyelectrolyte pair poly(styrenesulfonate)/poly(choline methacrylate) was used. The quality of the coatings was investigated by UV/vis spectroscopy, time-of-flight secondary ion mass spectrometry (ToF-SIMS), and X-ray photoelectron spectroscopy (XPS). The multilayer deposition on poly(propylene) (PP) and poly(ethylene terephthalate) (PET) was investigated in detail. On polar poly(ethylene terephthalate) supports, the regular growth of multilayer assemblies is evidenced. In contrast, on less polar supports, in particular on PP, the quality of the poly(styrenesulfonate)/poly(choline methacrylate) multilayers is inferior. However, if a hydrophobically modified poly(choline methacrylate) is employed instead, good quality multilayers are obtained even on PP. Thus, by appropriate choice of the polyelectrolytes used, even very hydrophobic and polar substrates become useful for the alternate adsorption technique.

1. Introduction

Very thin polymeric coatings can be realized by alternate adsorption of oppositely charged polyelectrolytes onto a charged substrate.[1−7] Neutron and X-ray reflectivity studies have shown that layer thicknesses down to 10 Å[1,6] and total layer numbers up to 50 and more could be successfully achieved.[4] However, most of the studies were realized on model, inorganic supports (e.g. quartz or charged silicon wafers), for technical reasons (need for a very flat substrate) and because it was thought that charged supports were required to initiate the process of multilayer buildup. Only singular reports[8,9] have investigated the deposition of alternate polyelectrolyte coatings on organic or polymer supports, which seem to be more promising candidates for future applications. In fact, the adsorption of polyelectrolytes on such substrates is not evident.

Multilayered assemblies composed of alternate polyelectrolytes have been recently investigated by surface analysis techniques: X-ray photoelectron spectroscopy (XPS) and time-of-flight secondary ion mass spectrometry (ToF-SIMS).[1,2] An important advantage of these techniques concerning the deposition on 'real world' supports is that they can be used whatever the substrate roughness is like, unlike X-ray reflectivity or ellipsometry. In our previous work, the combined use of SIMS and XPS brought information about the chemical structure and homogeneity of the top layers but also about the thickness (by the decay of the substrate signals) and, to some extent, about the structure (by the correlation between SIMS and XPS data) of the coatings.[1,2] It was shown that SIMS and XPS gave a quantitative determination of the sample thickness up to 50 Å and more. In comparison with XPS, the weaker sampling depth of the secondary ions in ToF-SIMS allows us to monitor very little changes of the average sample thickness. In addition, the agreement with X-ray reflectivity results for the determination of the thickness of a single polyelectrolyte layer was fairly good.[2] For thicker samples, information about the total amount of material deposited can be gained from UV/vis measurements.

In this paper, we report on the deposition of alternate polyelectrolyte coatings on various polymer substrates: poly(propylene), poly(isobutylene), poly(styrene), poly(methyl methacrylate), poly(ethylene terephthalate), poly(phenylene oxide), and poly(ether imide). The multilayers are constituted of alternately deposited poly(styrenesulfonate)/poly(choline methacrylate), a combination which has been successfully deposited on charged silicon supports.[2] In theory, the cohesion inside the multilayer assembly is ensured by the electrostatic attraction between the negative charges of the polyanion and the positive charges of the polycation. So far, the adsorption (and adhesion) of the first polyelectrolyte layers was ensured by electrostatic interactions, based on the use of charged supports. In the case of the uncharged polymer supports investigated, the adsorption of the first polycation layer is due to polar or to hydrophobic interactions, respectively. To improve the interaction with the apolar hydrophobic poly(propylene) supports, a hydrophobically modified copolymer of choline methacrylate was therefore studied, replacing the strongly hydrophilic parent poly(choline methacrylate).

* Corresponding author. Telephone: + 32 10 473582. Fax: +32 10 473452. E-mail: delcorte@pcpm.ucl.ac.be.

⊗ Abstract published in *Advance ACS Abstracts,* September 1, 1997.

(1) Delcorte, A.; Bertrand, P.; Arys, X.; Jonas, A.; Wischerhoff, E.; Mayer, B.; Laschewsky, A. *Surf. Sci.* **1996**, *366*, 149.
(2) Delcorte, A.; Bertrand, P.; Wischerhoff, E.; Laschewsky, A. *Proceedings of the Second International Conference on Polymer−Solid Interfaces*, Namur, August 1996, in press.
(3) Lvov, Y. M.; Decher, G. *Crystallogr. Rep.* **1994**, *39*, 696.
(4) Schmitt, J.; Grünewald, T.; Decher, G.; Pershan, P. S.; Kjaer, K.; Lösche, M. *Macromolecules* **1993**, *26*, 7058.
(5) Lvov, Y.; Ariga, K.; Ichinose, I.; Kunitake, T. *J. Am. Chem. Soc.* **1995**, *117*, 6117.
(6) Laschewsky, A.; Mayer, B.; Wischerhoff, E.; Arys, X.; Jonas, A. *Ber. Bunsen-Ges. Phys. Chem.* **1996**, *100*, 1033.
(7) Cochin, D.; Laschewsky, A.; Nallet, F. *Macromolecules*, submitted.
(8) Godinez, L. A.; Castro, R.; Kaifer, A. E. *Langmuir* **1996**, *12*, 5087.
(9) Brynda, E.; Houska, M. J. *Colloid Interface Sci.* **1996**, *183*, 18.

S0743-7463(97)00105-4 CCC: $14.00

Table 1. Solvents Used for the Spin Coating of the Polymer Supports

PIB	toluene
PS	toluene
PMMA	dichloromethane
PET-*co*-I	chloroform
PET	hexafluoro-2-propanol
PPO	toluene
PEI	chloroform

2. Experimental Section

2.1. Materials. The poly(propylene) (PP) film was kindly provided by Shell Research Louvain-la-Neuve (B). The high molar mass poly(isobutylene) (PIB) sample was purchased from Aldrich Chemie. The poly(styrene) (PS) and poly(methyl methacrylate) (PMMA) samples were obtained from Polyscience Polylab. Their molecular weights are respectively M_w(PS) = (1.25−2.5) × 10^5 and M_w(PMMA) = 10^5. The amorphous poly(ethylene terephthalate-*co*-isophthalate) (60−40) sample (PET-*co*-I) was purchased from ICI. The poly(2,6-dimethyl-*p*-phenylene oxide) sample (PPO) was purchased from Scientific Polymer Products (M_w = 5 × 10^5). The PET and the poly(ether imide) (PEI) were gifts from the laboratory POLY of the university (Pr. R. Legras and A. Jonas). The chemical formula of PEI is as follows:

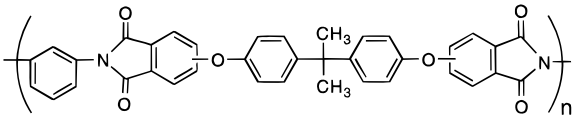

All the polymers were dissolved (2 wt % in solution) and spin-coated onto silicon wafers, except PP, which was received as a film. The solvents used for the polymer substrates are listed in Table 1. The silicon wafers were cleaned with hexane and ethanol prior to spin-coating.

The chemical formulas of the polyelectrolytes used for the multilayer buildup are indicated in Chart 1. The high molecular weight, branched poly(ethylene imine) (**1**) and poly(styrene-sulfonate) (**2**) were commercial products (Aldrich Chemie). The syntheses of poly(choline methacrylate) (**3**), of the copolymer **4**, and of the ionene-type polycation **5** were described elsewhere.[7,10] The polyelectrolytes were dissolved in ultrapure water (Millipore). The concentration of the solutions was 2 × 10^{-2} M.

2.2. Multilayer Assembly. All the samples described in sections 3.1 and 3.2 were first treated by dipping the polymer supports into a solution of poly(ethylene imine) (**1**).[3] The same routine has been used in the case of silicon substrates, allowing the adsorption of a primer polycation layer.[2] After the deposition of this primer layer, the samples were dipped successively into poly(styrene sulfonate) (**2**) and poly(choline methacrylate) (**3**) solutions. Samples with one to four **2**/**3** bilayers were built up.

The samples analyzed in section 3.3 were realized by replacing polycation **1** and/or **3** by the statistical copolymer **4**, containing a long alkyl residue (see Chart 1). Multilayer assemblies incorporating the ionene-type polycation **5**, bearing an azo-dye,[10] instead of polycation **3** were also realized.

In the following, the word "*layer*" will refer to one single polyelectrolyte layer (polyanion or polycation). In contrast, the expression "*deposition cycle*" will refer to the successive adsorption of one polyanion and one polycation layer, corresponding to the 'vertical' repeat unit of the multilayered assembly (this notation does not include the primer polycation layer).

2.3. Characterization Techniques. (*a) ToF-SIMS.* The system consists of a time-of-flight SIMS microprobe-microscope (Charles Evans & Assoc.) using a (5 kHz) pulsed Ga^+ beam (15 kV, 400 pA DC).[11] The Ga^+ beam is rastered over a 97 × 97 μm^2 area. The secondary ions are accelerated by a 3 kV voltage immediately after emission and deflected by three electrostatic analyzers in order to compensate for their initial energy and angular distributions. This results in a high mass resolution ($M/\Delta M$ > 5000 at mass 28 D), allowing the discrimination of

Chart 1. Structures of the Polyelectrolytes Used for the Multilayer Assemblies

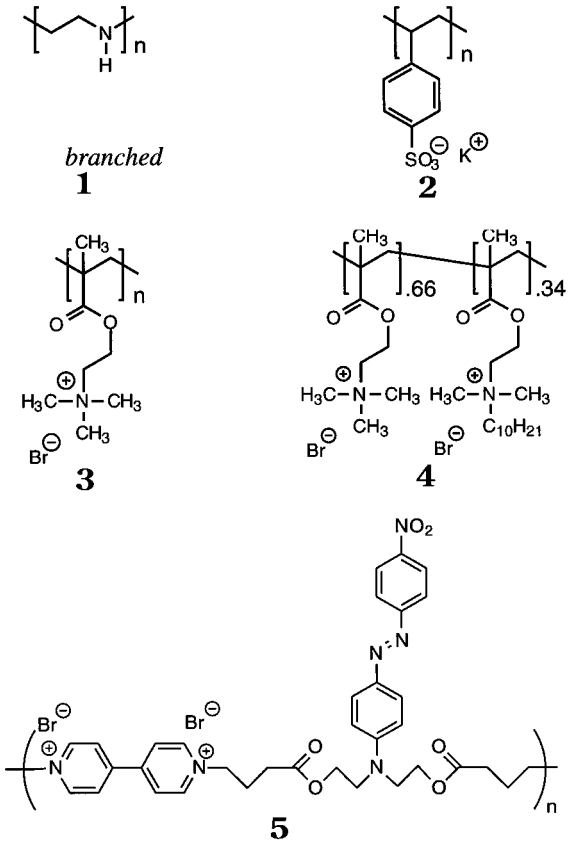

secondary ions with the same nominal mass. The mass spectrum is obtained by measuring the time-of-flight distribution of the ions from the sample surface to the detector. The total ion fluence for one spectrum acquisition is 10^{12} ions/cm^2, which is known to ensure static conditions in the case of polymer samples.[12] In the case of the PP film supports, the charge compensation of the samples was achieved with a pulsed electron gun (24 eV) and a grounded stainless steel grid covering the sample. No charge compensation was needed for the spin-coated polymer supports, as indicated by the high reproducibility and mass resolution of the analyses.

(b) XPS. The XPS equipment is a SSI-X-Probe (SSX-100/206 from Fisons)[13] with an aluminum anode (10 kV, 11.5 mA) and a quartz monochromator. The photoelectrons are energy-discriminated by an hemispherical analyzer and detected by a microchannel plate. The angle of detection in the usual configuration is 35° with respect to the sample surface. The analyzed surface is a spot of 1.37 mm^2. For this study, detailed scans of the main lines of each element found in the polyelectrolyte formulations were recorded. A Shirley type nonlinear background subtraction was used, and the peaks were decomposed by using a least square routine assuming a Gaussian/Lorentzian (85/15) function. The XPS atomic percentages (Table 2) were calculated from the peak area of each element, corrected by the corresponding sensitivity factor (C 1s, 1.0; O 1s, 2.49; N 1s, 1.68; S 2p, 1.79; Si 2p, 0.90).

(c) UV/vis. The UV/vis spectra of the multilayer assemblies on PP were taken with a SLM-AMINCO DW-2000 spectrophotometer in the double-beam mode. An uncovered substrate served as reference.

3. Results and Discussion

3.1. Overview of the Adsorption of Polyelectrolyte Multilayers on Polymers. The apolar PP and the polar

(10) Laschewsky, A.; Wischerhoff, E.; Kauranen, M.; Persoons, A. *Macromolecules*, submitted.

(11) Schueler, B. W. *Microsc. Microanal. Microstruct.* **1992**, *3*, 119.

(12) Delcorte, A.; Weng, L. T.; Bertrand, P. *Nucl. Instrum. Methods. Phys. Res., Sect. B* **1995**, *100*, 213.

(13) Weng, L. T.; Vereecke, G.; Genet, M. J.; Bertrand, P.; Stone, W. E. E. *Surf. Interface Anal.* **1993**, *20*, 179. Weng, L. T.; Vereecke, G.; Genet, M. J.; Rouxhet, P. G.; Stone-Masui, J. H.; Bertrand, P.; Stone, W. E. E. *Surf. Interface Anal.* **1993**, *20*, 193.

Table 2. XPS Atomic Percentages of the Elements before and after Deposition of the Coating 1/[2/3]$_3$ on Various Substrates

	C 1s	C 1s (O=C—O)	C 1s (shake up)	O 1s	N 1s	N 1s (N^+)	S 2p	Si 2p
			Before Deposition					
silicon	25.7	0	0	38.1	0.3	0	3.5	32.4
PP	100	0	0	0	0	0	0	0
PIB	100	0	0	0	0	0	0	0
PS	99.7	0	7.5	0.3	0	0	0	0
PMMA	72.1	14.08	0	27.9	0	0	0	0
PET-*co*-I	70.7	12.4	1.8	29.3	0	0	0	0
PET	70.0	12.0	0	30.0	0	0	0	0
PPO	89.1	0	7.6	10.9	0	0	0	0
PEI	82.5	6.1	3.9	13.0	4.5	0	0	0
			After Deposition					
silicon	58.3	4.0	0	25.2	4.1	3.4	2.9	9.5
PP	80.5	2.0	0	14.8	3.0	1.3	1.7	0
PIB	85.0	1.4	0	12.0	1.6	1.5	1.4	0
PS	76.0	2.4	1.0	18.2	3.3	2.8	2.5	0
PMMA	72.6	6.0	0	22.2	3.0	2.6	2.2	0
PET-*co*-I	72.6	6.3	0.8	22.1	3.0	2.6	2.3	0
PET	69.2	3.6	0	23.5	4.5	3.9	2.8	0
PPO	74.3	2.3	0.8	19.7	3.3	2.9	2.7	0
PEI	73.6	3.7	0	19.8	3.9	2.9	2.7	0

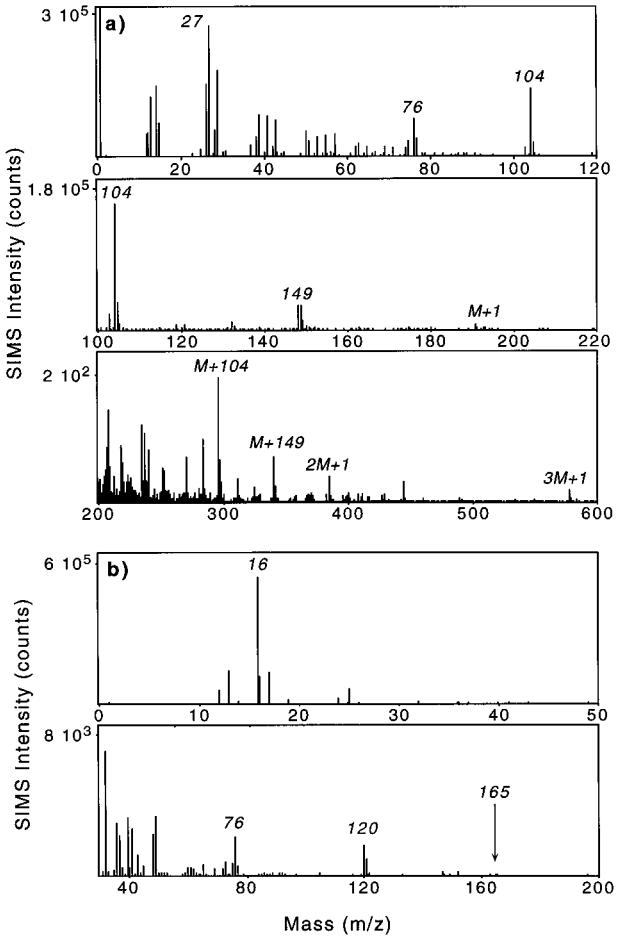

Figure 1. Positive (a) and negative (b) ToF-SIMS spectra of PET.

PET constitute two extreme cases of supports for the deposition of the multilayer **1**/[**2**/**3**]$_x$. They will be presented briefly in this section, to exemplify two opposite adsorption behaviors. The multilayer buildup on these two substrates will be investigated in detail in the next sections. The behavior of the other systems is intermediate between these two cases.

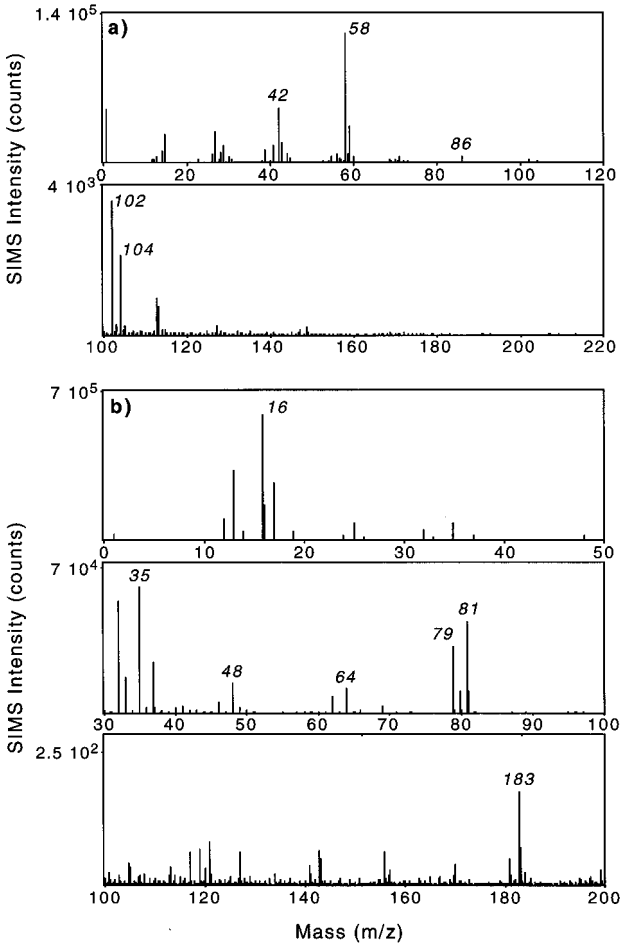

Figure 2. Positive (a) and negative (b) ToF-SIMS spectra of PET after deposition of the multilayer **1**/[**2**/**3**]$_3$.

The positive and negative secondary ion mass spectra of the pristine, semicrystalline PET are displayed in Figure 1. The most characteristic ions in the positive mode are $C_6H_4^+$ ($m/z = 76$), $C_6H_4CO^+$ ($m/z = 104$), $C_4H_6(COOH)$-CO^+ ($m/z = 149$), and the protonated monomer ($m/z = 193$).[14,15] Fragments larger than the monomer, including dimers and trimers, are also detected: m/z = M + 104, M + 149, 2M + 1, and 3M + 1, where M is the mass of the monomer ($m/z = 192$). The predominant hydrocarbon peaks at lower masses ($C_2H_3^+$, $C_2H_5^+$, $C_3H_3^+$, $C_3H_5^+$, etc.) correspond to the fragmentation of the ethylene and phenyl ring of PET, enhanced by the presence of oxygen atoms incorporated in the backbone. In the negative ion mass spectrum, the fingerprint of the PET structure is also clearly visible: $C_6H_4^-$ ($m/z = 76$), $C_6H_4COO^-$ and $C_6H_5COO^-$ ($m/z = 120-121$), $C_4H_6(COOH)COO^-$ ($m/z = 165$). The most intense peaks are due to CH^- and O^-.

The positive mass spectra of PP and PIB were presented previously.[12] PP exhibits few characteristic peaks,[14,15] except the hydrocarbon ions $C_4H_7^+$ ($m/z = 55$) and $C_5H_9^+$ ($m/z = 69$). For this reason, PIB was chosen as an alternative aliphatic hydrocarbon polymer in this study. The fingerprint ions of PIB are $C_6H_{11}^+$ ($m/z = 83$) and $C_7H_{13}^+$ ($m/z = 97$).[12,15]

After successive dipping into the polycation and polyanion solutions, in order to build the multilayer **1**/[**2**/**3**]$_3$ on

(14) Briggs, D.; Brown, A.; Vickerman, J. C. *Handbook of Static Secondary Ion Mass Spectrometry (SIMS)*; John Wiley: Chichester, 1989.

(15) Newman, J. G.; Carlson, B. A.; Michael, R. S.; Moulder, J. F.; Hohlt, T. A. In *Static SIMS Handbook of Polymer Analysis*; Hohlt, T. A., Ed.; Perkin-Elmer Corporation, Minnesota, 1991.

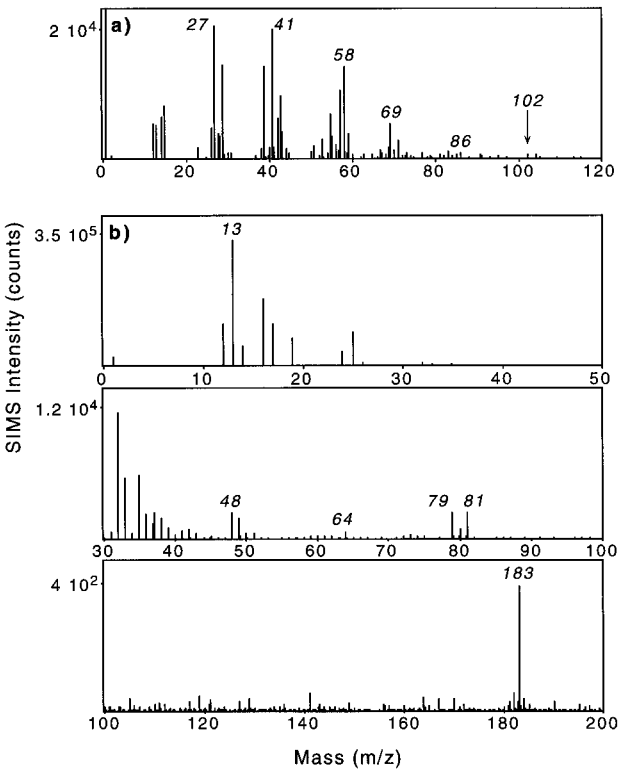

Figure 3. Positive (a) and negative (b) ToF-SIMS spectra of PP after deposition of the multilayer **1**/[**2**/**3**]$_3$.

the polymer support, the positive SI mass spectrum of PET looks completely different (Figure 2). Nitrogen-containing peaks are predominant: $C_2H_4N^+$ (m/z = 42), $C_3H_8N^+$ (m/z = 58), $C_5H_{12}N^+$ (m/z = 86), $C_5H_{12}NO^+$ (m/z = 102), and $C_5H_{14}NO^+$ (m/z = 104). They result mainly from bond scissions inside the pendant group of polymer **3**, indicating the efficient deposition of this polymer as the top layer of the assembly. Nevertheless, it is important to note that the ions $C_2H_4N^+$ (m/z = 42), $C_3H_8N^+$ (m/z = 58), and $C_5H_{10}N^+$ (m/z = 84) are the fingerprint ions of polymer **1**, too. The latter, probably emitted from the branched sites of polymer **1**, is very weak in the spectrum of polymer **3**. Therefore, it will be used in the following to monitor the decay of the primer polymer **1** signals after the deposition of subsequent polymer (**2**) and (**3**) layers. The negative ion mass spectrum of the same sample shows the presence of Cl and Br counterions (m/z = 35−37; 79−81) and of the underlying polymer **2** (sulfur-containing ions at m/z = 48, 64, 80, and 183). The peaks corresponding to the PET support are all very weak. The successive steps of the multilayer deposition on semicrystalline PET will be described in section 3.2.

The successful deposition of the multilayer **1**/[**2**/**3**]$_3$ on the apolar PP is less obvious than that on PET (Figure 3). Indeed, the intensity of the characteristic ions of polymer **3** (m/z = 42, 58, 86) is weak in comparison to the PP hydrocarbon ion intensities (m/z = 27, 41, 55, 69). The characteristic peaks of polymer **2** are present in the negative spectrum of the sample, but the ratio $I(O^-)/I(CH^-)$ is very small (<1) in comparison to that for the coated PET. This demonstrates that the amount of oxygen-containing polymers on the surface is small. However, the modification of the top surface of PP by adsorption of both polycation and polyanion chains is clearly indicated by the ToF-SIMS spectra.

The XPS spectra of PP and PET before and after the multilayer deposition confirm these observations. Parts a and b of Figure 4 show the detailed spectra of the pristine PP and PET. No contamination could be detected in the general spectrum of the pristine PP and PET. From the pristine PET spectra, the ratio O/C is 0.43 (0.40 from the chemical structure), and the ratio between the two types of oxygen, O=C/O−CH_2, is equal to 0.98. The spectra are very similar to those published in the literature,[16,17] which indicates the purity of this polymer surface.

After deposition, the PP spectra become complex (Figure 4c). Oxygen, nitrogen, and sulfur are introduced on the surface, but the amount of characteristic functionalities remains small. In particular, the fraction of carbon bound to two oxygen atoms (O=C−O), the fraction of nitrogen corresponding to the charged group (N^+), and the total percentage of sulfur (S 2p), which are easily identified, are all below 2 atomic % of the total (Table 2). Considering the chemical structure of the **2**/**3** polymer pair, these should reach 4 atomic % of the total for a dense layer adsorption. Conversely, the total percentage of carbon is above 80 atomic %, whereas it should be close to 70 atomic %, according to the **2**/**3** pair structure.

The behavior of semicrystalline PET is different. After deposition, the atomic fractions of the characteristic groups are close to 4 atomic %, except the sulfur atomic percentage (2.8 atomic %). Similar trends were observed on silicon.[2] This could be explained by the layered structure of the coating, in which the sulfur-containing layer of polymer **2** is buried under the top layer of polymer **3**. In addition, the carbon and oxygen fractions are close to the calculated values (Table 2).

The atomic fractions of each element found in the XPS spectra of silicon, PP, PIB, PS, PMMA, PET, PET-*co*-I, PPO, and PEI, before and after deposition of the multilayer **1**/[**2**/**3**]$_3$, are displayed in Table 2. These data enable a first evaluation of the coating quality for the different polymer supports. The cases of the silicon,[2] PP, and semicrystalline PET supports were described earlier. For the other substrates, the atomic fractions before deposition are close to the expected values (no contamination could be detected). After three deposition cycles, the quality of the coating on PIB is even worse than that on PP (high carbon fraction and low atomic percentages of the **2**/**3** characteristic functionalities).

The substrate signals remain present after deposition in the case of PS, PMMA, PET-*co*-I, and PPO (significant shake-up peak in the cases of PS and PPO; intense O=C−O contribution to the carbon peak in the cases of PMMA and PET-*co*-I). This could be due either to an incomplete substrate coverage (roughness, defects, etc.) or to a very thin coating. The thickness of a similar coating deposited on silicon has been evaluated by comparing the XPS and SIMS intensities of the substrate signals for a set of samples with increasing layer number.[2] For three **2**/**3** layer pairs, the thickness obtained from the XPS and SIMS data was close to 50 Å. As this value is comparable to the XPS mean free path of carbon C 1s, the attenuated signal of the C 1s substrate photoelectrons after passing through a similar coating would reach ~10−20% of its initial value ($I = I°$ exp $50/(\lambda \cos \theta)$, where λ is the mean free path of the photoelectrons and θ is the angle between the detector and the normal to the sample surface, 55° in our system). In the case of PS, PMMA, PET-*co*-I, and PPO, the intensities of the contributions of the substrate photoelectrons to the C 1s spectrum are close to these values, which therefore do not exclude a uniform coverage of the polymer support. In addition, the nitrogen and sulfur fractions are well above 2%, indicating a better adsorption

(16) Boulanger, P.; Pireaux, J. J.; Verbist J. J.; Delhalle, J. *J. Electron Spectrosc. Relat. Phenom.* **1993**, *63*, 53.
(17) Beamson, G.; Clark, D. T.; Hayes, N. W.; Law, D. S.-L.; Siracusa, V.; Recca, A. *Polymer* **1996**, *37*, 379.

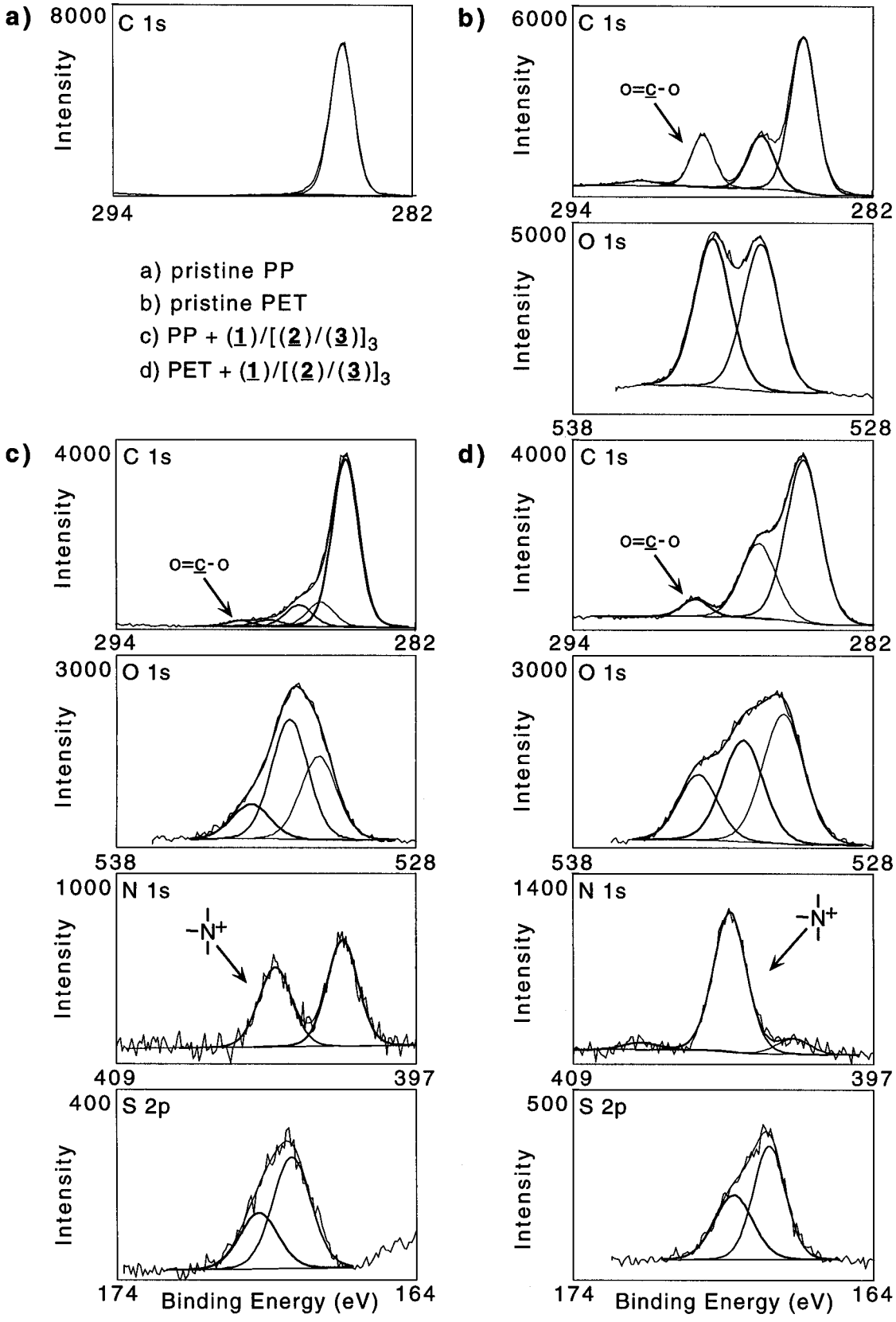

Figure 4. XPS. Detailed spectra of the main lines of each element found in (a) PP; (b) PET; (c) PP coated with the multilayer **1**/[**2**/**3**]$_3$; (d) semicrystalline PET coated with the multilayer **1**/[**2**/**3**]$_3$.

of the coating than that for PP and PIB subtrates. This remark is valid in the case of PEI too.

The absolute intensities of the polyelectrolyte secondary ions are shown in Figure 5 for the nine different substrates, including silicon. The same trends are observed if these values are normalized by the total spectrum intensities. As already mentioned, the weaker intensities are observed with PP and PIB substrates, whereas the higher intensities correspond to PPO and semicrystalline PET substrates. Intermediate intensities are observed for treated silicon, PS, PMMA, PET-*co*-I, and PEI substrates. As the regular multilayer buildup has been demonstrated in the

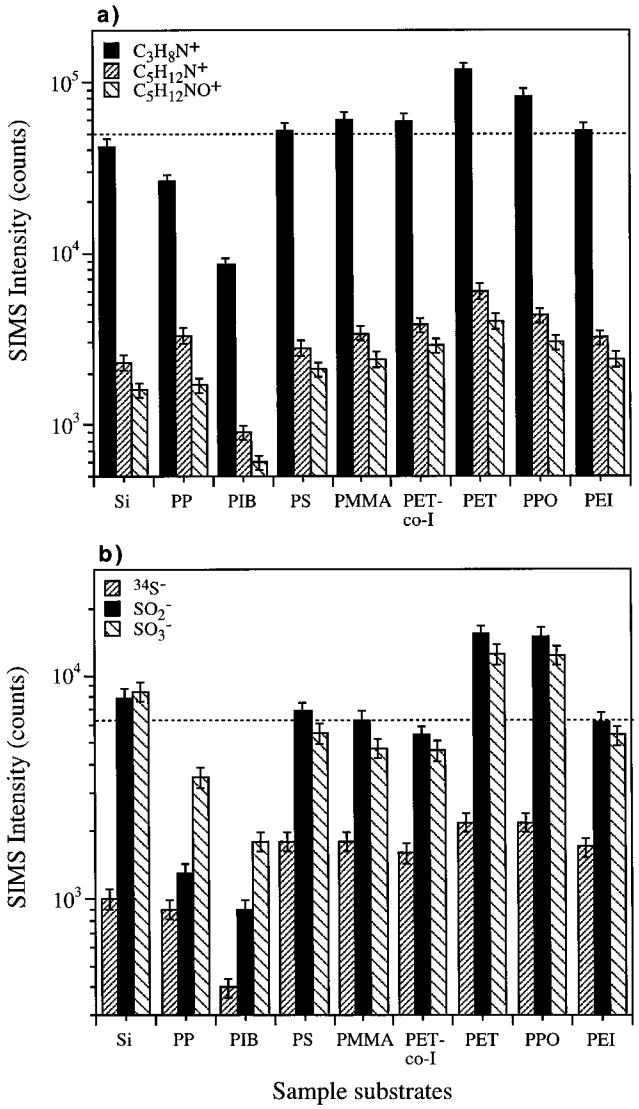

Figure 5. ToF-SIMS. Absolute intensity of the most characteristic ions of polymers **2** and **3** after deposition of the assembly **1**/[**2**/**3**]$_3$ on various substrates.

case of the treated silicon support,[2] these intermediate values suggest once more that the alternating deposition occurs on such substrates, too.

The decay of the substrate ion intensities is also indicative of the coating quality. With three **2**/**3** layers deposited on silicon, the Si^+ ion intensity was reduced by a factor of ~30.[2] Assuming that the attenuation of molecular ions inside the coating is stronger than the one of atomic ions,[1] one should expect at least a similar decrease for polymer substrates if the coating quality is comparable. Indeed, previous works have shown that large molecular ions have a very limited emission depth (<10 Å).[1] In addition, the intensity variation of the large fingerprint secondary ions sputtered from the polymer substrate is more significant than the one of small or hydrocarbon ions which could be produced inside the coating. Figure 6 shows the evolution of the substrate ion intensities for the different polymer substrates, after the deposition of the assembly **1**/[**2**/**3**]$_3$. Once more, PP and PIB exhibit anomalous behavior: the absolute intensity of the characteristic hydrocarbon ions is even increased by a factor of ~2 after deposition of the coating. Such an increase of the secondary ion yields is probably due to the introduction of heteroelements (oxygen and nitrogen) on the surface, which improves the ionization probability of the sputtered particles. A similar phenomenon has been observed with plasma-treated hydrocarbons.[18] The normalization of these peaks to the intensity of an uncharacteristic hydrocarbon ion ($C_2H_3^+$) allows us to overcome this matrix effect: the ratios $I(C_4H_7^+)/I(C_2H_3^+)$ and $I(C_5H_9^+)/I(C_2H_3^+)$, which are respectively equal to 0.76 ± 0.02 and 0.61 ± 0.03 for pristine PP, are reduced by a factor 1.5−2 after deposition (respectively 0.51 ± 0.05 and 0.31 ± 0.04). For the other polymers, the intensity of the most characteristic substrate ions is reduced by a factor of ~10 at least: ~10 for PS, PMMA, and PEI, ~30 for PET-*co*-I and PPO, and ~400 for semicrystalline PET. As was the case for PP, the evolution of the fingerprint ions is probably the result of two different effects: the attenuation of the signal due to the coverage of the substrate and the variation of the ionization probability due to the modification of the chemical environment. The second effect should be weak with oxygen-containing polymer supports (PMMA, PET, PPO, and PEI). It is more difficult to isolate the relative contributions of these two effects in the case of the PS substrate. The limited variation observed for PS, PMMA, PET-*co*-I, PPO, and PEI, even for very large molecular ions, might suggest that the coverage is not perfect. This could be due either to a large roughness of the coating, of the same order of magnitude as the multilayer thickness, or to local defects where the substrate is not covered. Still, SIMS as well as XPS results show that important amounts of both polyelectrolytes **2** and **3** are deposited in these cases, too.

3.2. Adsorption on PET. The results discussed before indicate that semicrystalline PET is the most suitable polymer candidate for the deposition of the multilayer system **1**/[**2**/**3**]$_x$. After three cycles, the amount of material deposited is even higher on semicrystalline PET than on treated silicon supports.[2] For this reason, a step by step study of the deposition in the system PET + **1**/[**2**/**3**]$_x$ was performed in order to improve the understanding of the adsorption mechanism.

The variation of the XPS atom percentages of the elements after each deposition step, up to four **2**/**3** deposition cycles, is displayed in Figure 7. The data obtained for the PET substrate are compared with those obtained on treated silicon wafers. All the atomic fractions (except for sulfur) tend to the stoichiometric values of the **2**/**3** layer pair (indicated by the horizontal lines). The lack of sulfur has been explained by the attenuation of the S 2p photoelectrons in the polymer **3** top layer.[2] The variations of the carbon and oxygen atomic percentages are weak, due to the presence of these elements in the substrate as well as in the coating (Figure 7a). The oxygen content decreases from ~30 to ~22 atomic %, which corresponds respectively to the percentages expected for pristine PET and for the **2**/**3** assembly. The regular decay of the substrate signal is even more obvious with the O=C—O component of the C 1s peak (Figure 7b). Parallel to the decay of the substrate peak intensities, Figure 7b and c shows the increase of the signals related to the coating. The intensity of the peaks N 1s (N^+) and S 2p increases linearly up to three **2**/**3** cycles and saturates after this point, which indicates that the contribution of the substrate to the atomic percentage of the elements becomes negligible. In other words, the substrate photoelectrons cannot leave the coating anymore.

The comparison with the treated silicon substrate indicates that the convergence toward the stoechiometric values of the nitrogen fraction corresponding to charged

(18) Léonard, D.; Bertrand, P.; Scheuer, A.; Prat, R.; Hommet, J.; Le Moigne, J.; Deville, J. P. *J. Adhes. Sci. Technol.* **1996**, *10*, 1165.

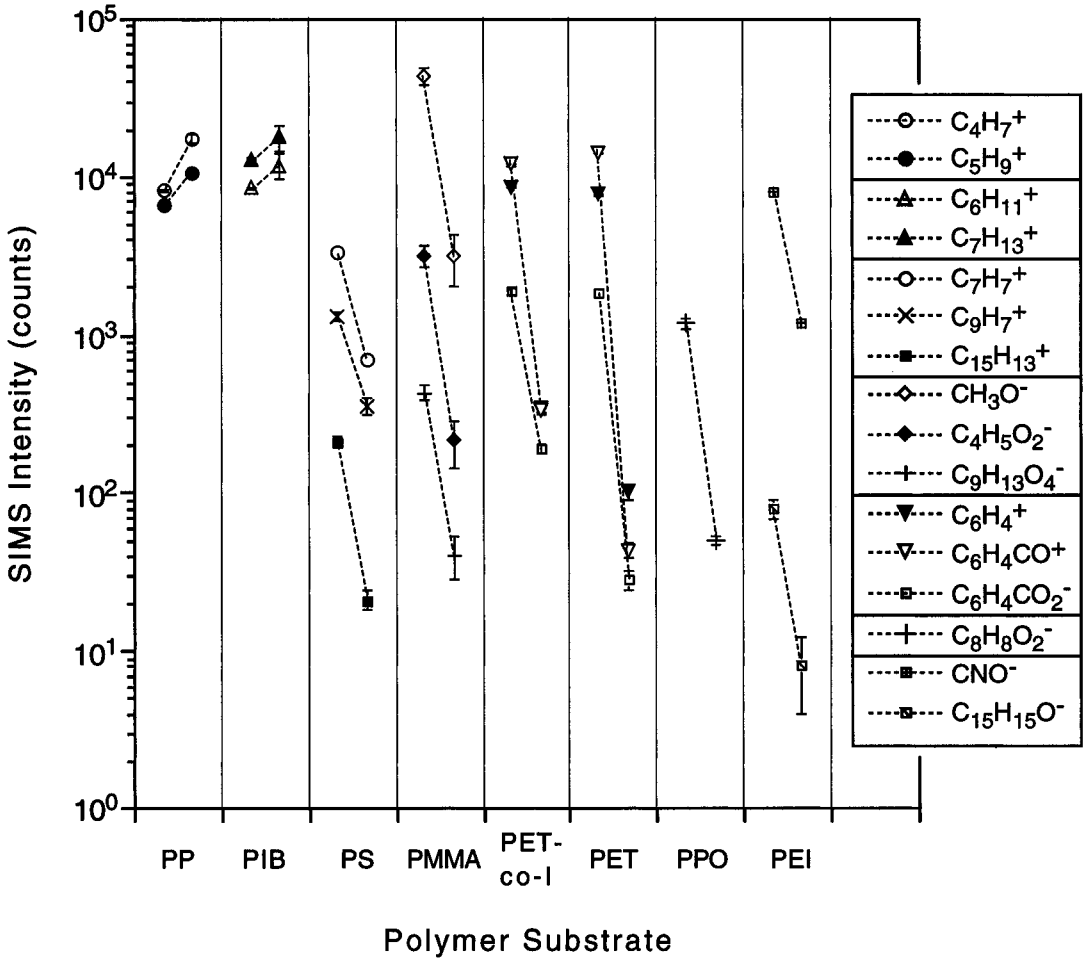

Figure 6. ToF-SIMS. Absolute intensity of the fingerprint ions of the polymer supports PP, PIB, PS, PMMA, PET-*co*-I, PET, PPO, and PEI *before* and *after* coating with the multilayer **1**/[**2**/**3**]$_3$. The dashed lines show the extent of the variation.

groups (N^+) is faster in the case of the PET substrate: the N^+ fraction is systematically higher. The anomalous evolution of the S 2p line with the cycle number in the case of silicon support can be understood considering the XPS atomic fractions of bare silicon in Table 2: sulfur is already present at the surface of the substrate before any deposition.

The C 1s (O=C—O) is the sum of two components: one is related to the carbonyl functionalities of PET and the other is due to the methacrylate group of polymer **3**. The fraction due to the first component can be calculated from the following equation:

$$I[\text{C 1s (O=C—O; PET)}] = I[\text{C ls (O=C—O)}] - \left(\frac{I[\text{C ls (O=C—O)}]}{I[\text{N ls (N}^+\text{)}]}\right)^{\infty} \times I[\text{N ls (N}^+\text{)}] \quad (1)$$

where I[C 1s (O=C—O)] is the absolute C 1s intensity due to carbonyl groups, I[C 1s (O=C—O; PET)] is the component due to PET, I[N 1s (N^+)] is the absolute intensity of nitrogen (N 1s) due to the charged group of **3**, and

$$\left(\frac{I[\text{C ls (O=C—O)}]}{I[\text{N ls (N}^+\text{)}]}\right)^{\infty}$$

is the absolute intensity ratio between the carbonyl group signal (C 1s) and the charged nitrogen signal (N 1s) when the intensity due to the substrate is negligible.

$$\left(\frac{I[\text{C ls (O=C—O)}]}{I[\text{N ls (N}^+\text{)}]}\right)^{\infty}$$

can be approximated with the XPS values corresponding to the sample PET + **1**/[**2**/**3**]$_4$. The variation of I[C 1s (O=C—O; PET)] with the layer number is shown in Figure 8. A very similar curve shape is obtained when the experimental value

$$\left(\frac{I[\text{C ls (O=C—O)}]}{I[\text{N ls (N}^+\text{)}]}\right)^{\infty}$$

is replaced by the ratio of the XPS sensitivity factors of nitrogen N 1s and carbon C 1s in eq 1 (which corresponds to the justified assumption that the ratio of the detected concentrations N 1s (N^+):C 1s (O=C—O) is 1:1). This is true even if the two values are slightly different in practice:

$$\left(\frac{I[\text{C ls (O=C—O)}]}{I[\text{N ls (N}^+\text{)}]}\right)^{\infty} = 0.50$$

and the ratio of the elemental sensitivity factors ESF(C 1s)/ESF(N 1s) = 0.59. Assuming that the thickness of the coating is uniform and that the inelastic mean free path λ(C 1s) = 43 Å,[19,20] the mean thickness of one layer of the

(19) Seah, M. P.; Dench, W. A. *Surf. Interface Anal.* **1979**, *1*, 2.

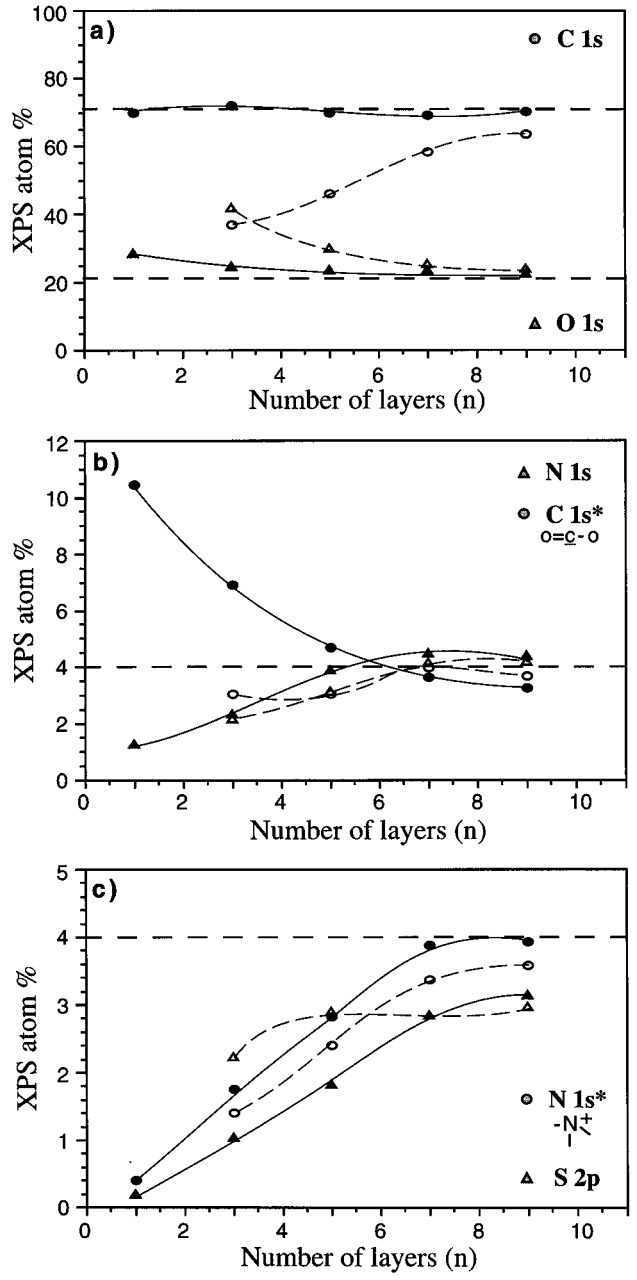

Figure 7. XPS. Evolution of the atomic percentages of the elements as a function of the layer number for the multilayer **1**/[**2**/**3**]$_x$ coated on PET (full symbols and full lines) and silicon (empty symbols and dashed lines): (a) C 1s and O 1s lines; (b) C 1s (O=C−O) component (see text) and N 1s line; (c) N 1s (N^+) component (see text) and S 2p line.

assembly **1**/[**2**/**3**]$_x$ can be deduced from the fitting of the decay of *I*[C 1s (O=C−O; PET)] by an exponential law. The best fit gives a thickness close to 12 Å for one single layer, which is more than the value obtained for the same assembly deposited on silicon. However, the shape of the curve in Figure 7 is not strictly exponential, suggesting that the layer thickness increases with the number of deposition cycles. An exponential line based on the first three data points (0−2 layers) would give a single layer thickness of ∼5 Å whereas another fit based on the three last data points (3−7 layers) would indicate a thickness of ∼16 Å.

The variation of the SIMS intensities as a function of the layer number for the series PET + **1**/[**2**/**3**]$_x$ is shown

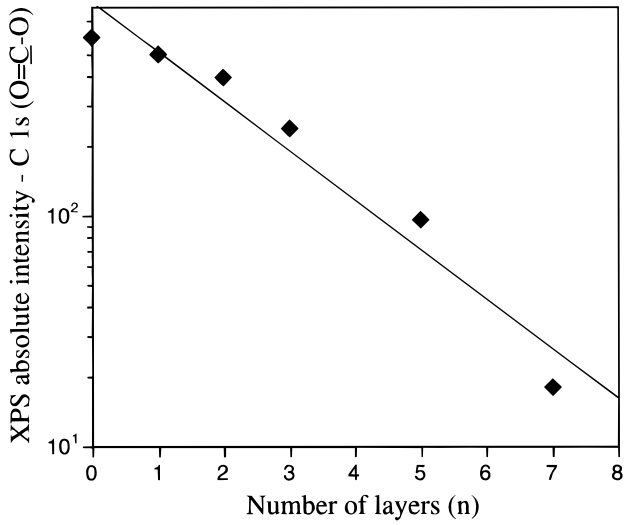

Figure 8. XPS. Absolute intensity variation as a function of the layer number of the C 1s(O=C−O) component related to PET (see text).

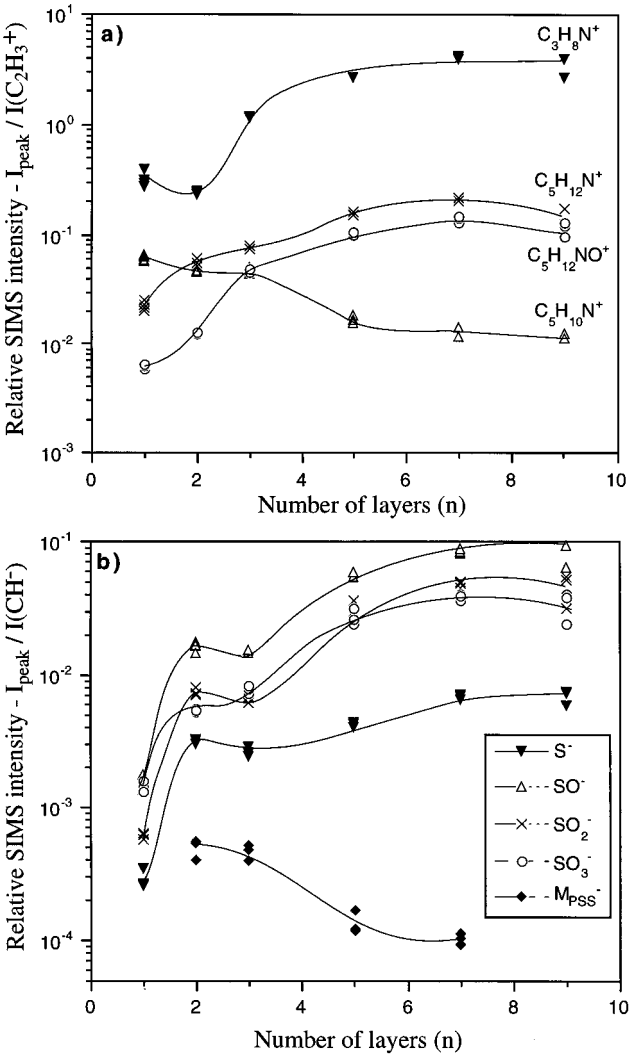

Figure 9. ToF-SIMS. Absolute intensity of the polyelectrolyte fingerprint peaks as a function of the layer number: (a) polycation **3** (and **1**) peaks; (b) polyanion **2** peaks.

in Figures 9 and 10. The saturation of the peaks corresponding to polymer **3** is reached within two **2**/**3** deposition cycles (five polyelectrolyte layers; Figure 9a), whereas three or four cycles were necessary to saturate the intensity of the photoelectrons emitted from the coating

(20) Horr, T. J.; Ralston, J.; Smart, R. St. C. *Colloids Surf., A* **1994**, 92, 277.

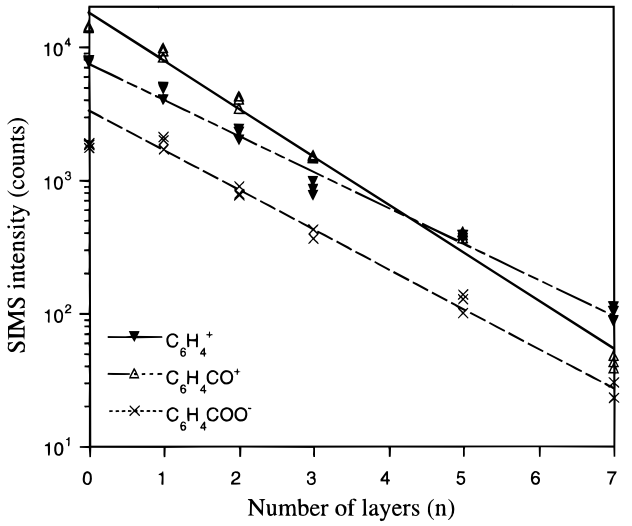

Figure 10. ToF-SIMS. Absolute intensity variation of the PET fingerprint peaks as a function of the layer number.

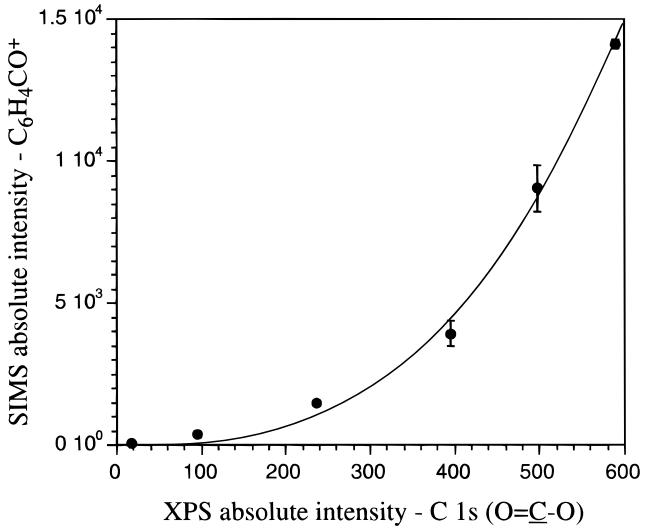

Figure 11. Correlation between the intensities of the substrate fingerprint ion $C_6H_4CO^+$ peak (ToF-SIMS) and the C 1s (O=C−O) component related to PET peak (XPS).

(seven to nine polyelectrolyte layers; Figure 7). This is due to the more limited emission depth of the molecular secondary ions.[1] Within these ions, $C_5H_{12}NO^+$ is the most characteristic of the structure of polymer **3**, whereas $C_3H_8N^+$, $C_5H_{10}N^+$, and $C_5H_{12}N^+$ are also emitted from the primer polymer **1** layer. In particular, the emission of $C_5H_{10}N^+$ is mainly due to the primer layer. The intensity of this ion decreases with the number of cycles to reach a constant value, which is six times lower than the initial intensity observed for polymer **1**. It is worth noting that the decay of this signal is weak after the first **2**/**3** pair deposition, whereas it is much more pronounced after the second deposition cycle. This is corroborated by the evolution of the ion intensities of polymer **3** (not saturated with the first polymer **3** layer). Also, this confirms the XPS results concerning the limited apparent thickness of the first layers. This could be due to an incomplete coverage or to the deposition of thinner starting layers. It will be shown in the following that the roughness of the coatings remains much smaller than their total thickness, which excludes the first possibility.

The variation of the polymer **2** signals is also informative (Figure 9b). The monomer ion intensity (M_2^-) is weakly attenuated by the top layer of polymer **3** in the sample **1**/**2**/**3**, but the attenuation is more and more pronounced when the number of deposition cycles increases. As most of the M_2^- ion intensity is due to the polymer **2** which lays just under the polymer **3** top layer (very weak emission depth[2]), this ion is attenuated in the very last polymer **3** layer only. Thus, the decay of M_2^- is consistent with an increasing thickness of the polymer **3** layer with the cycle number. In contrast, the intensity of the small SO_x ions increases with the cycle number and saturates with three or four deposition cycles (seven to nine polyelectrolyte layers), depending on the ion considered. These very different behaviors are most probably related to the larger sampling depth of the small molecular ions in comparison to the larger ones. As the total amount of polymer **2** increases with the layer number, these ion intensities increase to a certain extent. They reach a plateau when the total thickness of the coating is larger than their information depth. An alternative explanation would be that a higher amount of polymer **2** is deposited in higher layer numbers.

The fast, regular decay of the PET ion intensities as a function of the polyelectrolyte layer number (Figure 10) is in agreement with the above XPS results. In addition, the substrate secondary ions are much more sensitive to little variations of the coating thickness than the substrate photoelectrons:[1] with seven polyelectrolyte layers on the PET substrate, the intensity of the substrate photoelectrons is reduced by a factor of ∼30 (Figure 8), whereas the $C_6H_4CO^+$ absolute intensity is reduced by a factor of ∼400 (Figure 10). It has been shown that the variation of the substrate ion intensities in SIMS is an exponential function of the coating thickness,[1] as is the case for the photoelectrons in XPS. In SIMS, the intensity of the substrate ions can be written $I_{SIMS} = I°_{SIMS} \exp(-d/\lambda_{SIMS})$, where d is the coating thickness and λ_{SIMS} is the mean emission depth of the secondary ions. With the same assumptions as before (uniform coating thickness and inelastic mean free path λ(C 1s) = 43 Å), the mean emission depth of the PET ions can be calculated with the following relation:[1]

$$I_{SIMS} = \left(\frac{I°_{SIMS}}{I°_{XPS}}\right)^{\lambda_{XPS}/\lambda_{SIMS}} \times (I_{XPS})^{\lambda_{XPS}/\lambda_{SIMS}} \qquad (2)$$

This equation indicates that the correlation between SIMS and XPS substrate signals is a power function with an exponent $\lambda_{XPS}/\lambda_{SIMS}$, in the case of a uniform coating thickness. Conversely, a linear relationship between the SIMS and XPS intensities would suggest that the observed substrate signals are mainly due to the contribution of uncovered substrate areas which are reduced step by step by the successive polyelectrolyte depositions. The correlation between the $C_6H_4CO^+$ and the C 1s (O=C−O; PET) absolute intensities (Figure 11) shows that the effect of the coating thickness is predominant (power function). The ratio $\lambda_{XPS}/\lambda_{SIMS}$ given by the fitting is 2.9, which corresponds to a mean emission depths $\lambda_{SIMS}(C_6H_4CO^+)$ close to 8 Å. The calculated mean emission depth λ_{SIMS}-$(C_6H_4^+)$ and $\lambda_{SIMS}(C_6H_4COO^-)$ are close to 8 Å, too. However, the mean emission depths given by the simple power law are maximum values, due to the hypothesis of uniform thickness. The introduction of surface roughness would lead to a much more complex relation instead of eq 2 and to an overestimation of λ_{SIMS} by this equation. Nevertheless, the observed correlation between SIMS and XPS results with one to four deposition cycles shows that the coating thickness is much larger than the roughness in the case of the semicrystalline PET substrate, which is not clear with the other polymer supports (see section 3.1).

Table 3. XPS Atomic Percentages of the Elements after Deposition of Various Coatings on PP[a]

	C 1s	C 1s (O=C—O)	O 1s	N 1s	N 1s (N^+)	S 2p
3/[**2**/**3**]$_3$	80.6 (71)	2.5	15.0 (21)	2.5 (4.2)	1.8	1.9 (4.2)
4/[**2**/**3**]$_3$	86.4	1.6	10.2	2.0	1.6	1.5
4/[**2**/**4**]$_3$	78.1 (74)	1.6	15.9 (18)	2.7 (3.7)	2.5	3.2 (3.7)
4/[**2**/**5**]$_4$	76.0	2.1	14.9	7.1	2.3	2.0

[a] The stoichiometric values are indicated in parentheses (see text).

The interpretation of the results obtained with the coated PET supports can be summarized in two points: (i) the roughness of the coatings is small with respect to their thickness; (ii) the thickness of the layers increases with increasing number of deposition cycles. The small thickness calculated for the first layers suggests that the chains lie flat on the surface, whereas the nonlinear increase of the amount of material deposited indicates a gradual change of the chain conformation, leading to the formation of coils, which has already been reported for alternate polyelectrolyte coatings.[3,4] This could be due to the combined influence of the nonspecific interactions leading to the first layer adsorption together with the evolution of the net surface charge density at each deposition step. The latter is indeed closely related to the characteristics of the supports, uncharged in our case, and to the conformation of the layers adsorbed during the preceding deposition steps.[21] The fact that the equilibrium is not reached within three deposition cycles is in agreement with the results published by other groups, too.[3,4]

3.3. Adsorption on PP. It has been shown in section 3.1 that the deposition of multilayer assemblies **1**/[**2**/**3**]$_x$ on PP was more difficult than that on PET. This is probably due to the lack of interaction between the first polycation layer **1** and the hydrophobic polyolefin substrate. To improve the quality of the assembly, different primer layers were tested: (i) polymer **3** and (ii) a statistical copolymer based on choline methacrylate with an analogous monomer bearing a long aliphatic residue (see Chart 1; polymer **4**). Such polymers have a tendency to undergo hydrophobic association and to be surface active in aqueous solution.[7] Due to the affinity of this long alkyl residue to the PP surface, an improvement in the deposition of the first layer was expected, as well as a uniform distribution of the positive charges on the surface, leading to a better initiation of the multilayer buildup.

The XPS elemental composition of the samples after deposition of the multilayers **3**/[**2**/**3**]$_3$ and **4**/[**2**/**3**]$_3$ is displayed in Table 3. The low fraction (<2 atomic %) of the characteristic groups (N 1s (N^+); S 2p) indicates that the quality of the deposition is not drastically improved by modifying the primer polycation layer. Unexpectedly, the **4**/[**2**/**3**]$_3$ assembly seems to be of even worse quality than the **1**/[**2**/**3**]$_3$ and **3**/[**2**/**3**]$_3$ samples. This is confirmed by the ToF-SIMS characteristic ion intensities (Table 4). The intensity of the polymer **3** ions remains rather weak, but the more convincing observation is related to the SO_x^- ions sputtered from polymer **2**: in comparison with the 'intermediate' deposition cases of section 3.1 (on PS, PMMA, PET-*co*-I, and PEI), these ion intensities are reduced by a factor of 2 for the assembly **3**/[**2**/**3**]$_3$ and by a factor of 5−10 for the assembly **4**/[**2**/**3**]$_3$, which in fact corresponds to the poor deposition cases depicted in section 3.1 (on PP and PIB). It is hard to obtain quantitative information by looking at the PP substrate ion intensities for two reasons: (i) The effect of the introduction of heteroatoms on the surface on the ionization probability of these ions is difficult to determine; (ii) a certain amount of these ions could be sputtered from the coating itself (especially from the long alkyl chain of polycation **4**). To overcome the first effect, the substrate ion intensities were normalized in Table 4 by the intensity of an uncharacteristic, hydrocarbon ion ($C_2H_3^+$). After deposition of the assemblies **3**/[**2**/**3**]$_3$ and **4**/[**2**/**3**]$_3$, the normalized intensity of $C_5H_9^+$ is reduced by a factor of 2, which is qualitatively similar to the case of the assembly **1**/[**2**/**3**]$_3$.

Table 4. Absolute Intensity of the Most Characteristic Ions of the Coatings and of the PP Substrate after Deposition of Various Polyelectrolyte Coatings (10^3 counts)

	3/[**2**/**3**]$_3$	**4**/[**2**/**3**]$_3$	**4**/[**2**/**4**]$_3$
Positive Ions			
$C_3H_8N^+$	36 ± 4	15 ± 0.7	43 ± 3
$C_5H_{12}N^+$	2.3 ± 0.1	1.0 ± 0.1	1.6 ± 0.1
$C_5H_{12}NO^+$	1.6 ± 0.3	0.7 ± 0.1	0.7 ± 0.1
$C_{12}H_{26}N^+$	0	0.1 ± 0.05	1.2 ± 0.2
$C_{14}H_{30}N^+$	0	0.03 ± 0.01	0.26 ± 0.02
$C_{14}H_{30}NO^+$	0	0.04 ± 0.02	0.29 ± 0.03
$C_4H_7^+/C_2H_3^+$ *(PP: 0.76 ± 0.02)*	0.48 ± 0.02	0.50 ± 0.02	0.28 ± 0.01
$C_5H_9^+/C_2H_3^+$ *(PP: 0.61 ± 0.03)*	0.28 ± 0.01	0.34 ± 0.02	0.12 ± 0.01
Negative Ions			
S^-	0.9 ± 0.1	0.6 ± 0.1	2.0 ± 0.2
SO^-	6.3 ± 0.4	1.8 ± 0.3	12 ± 2
SO_2^-	2.7 ± 0.1	0.7 ± 0.1	6.4 ± 0.9
SO_3^-	2.6 ± 0.1	1.3 ± 0.2	4.7 ± 0.5

In contrast, the replacement of polymer **3** by polymer **4** at each deposition step gives very interesting results. The XPS results concerning this sample are summarized in Table 3. The stoichiometric values for the layer pair **2**/**4** are indicated in parentheses. They were calculated assuming that one polymer **2** repeat unit corresponds to one comonomer unit of the copolymer **4** and that the respective amount of the two monomers in copolymer **4** was two choline methacrylate units for one 'C_{10} residue' unit. The elemental fractions are much closer to the stoichiometric values than in the other cases of deposition on PP (the nitrogen and sulfur concentrations are higher). This time, the difference between the measured and calculated values is similar to the one observed with the deposition of **1**/[**2**/**3**]$_3$ on PS, PMMA, PET-*co*-I, PPO, and PEI (intermediate cases). ToF-SIMS confirms this result. In addition to the characteristic ions of the choline methacrylate comonomer, rather intense contributions of similar ions with a long alkyl chain are observed in the ToF-SIMS spectra of the multilayer **4**/[**2**/**4**]$_3$. They peak at $m/z = 184$ ($C_{12}H_{26}N^+$), $m/z = 212$ ($C_{14}H_{30}N^+$), $m/z = 228$ ($C_{14}H_{30}NO^+$), $m/z = 230$ ($C_{14}H_{32}NO^+$), and $m/z = 298$ ($C_{19}H_{40}NO^+$). Due to the different nature of the polycation, the intensity of the nitrogen-containing ions observed with the assembly **4**/[**2**/**4**]$_3$ cannot be directly compared to the values reported in Figure 5 for the other samples. However, the polymer **2** signals give information about the coating quality. With the assembly **4**/[**2**/**4**]$_3$, the SO_x^- ion intensities are close to the values obtained for the deposition of **1**/[**2**/**3**]$_3$ on PS, PMMA, PET-*co*-I, PPO, and PEI. In addition, the normalized intensity of the substrate ion $C_5H_9^+$ is five times weaker for the sample **4**/[**2**/**4**]$_3$ than for pristine PP. As the amount of $C_5H_9^+$ emitted by the alkyl chains of the copolymer should be significant (see for example the ToF-SIMS spectrum of hexatriacontane[18] or polyethylene[12]), the important reduction of this signal confirms that the deposition is efficient.

The XPS and Tof-SIMS results are corroborated by UV/vis spectroscopy: the absorbance at 229 nm caused by

(21) Arys, X.; Jonas, A. M.; Laguitton, B.; Legras, R.; Laschewsky, A.; Wischerhoff, E. *Prog. Org. Coat.*, submitted.

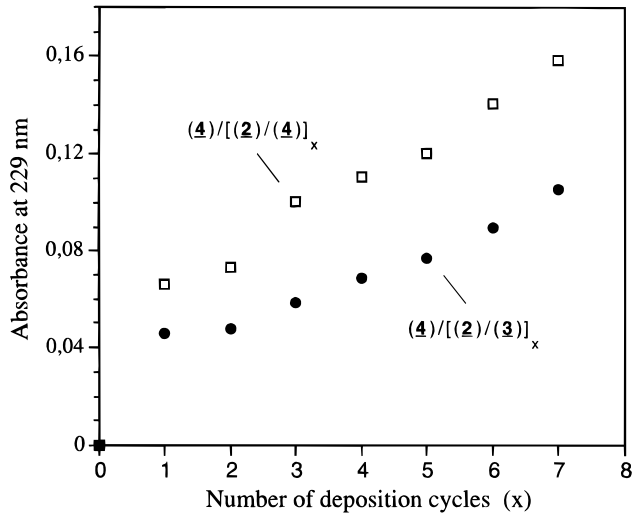

Figure 12. UV/vis. Evolution of the absorbance at 229 nm as a function of the number of deposition cycles for the assemblies **4**/[**2**/**3**]$_x$ and **4**/[**2**/**4**]$_x$.

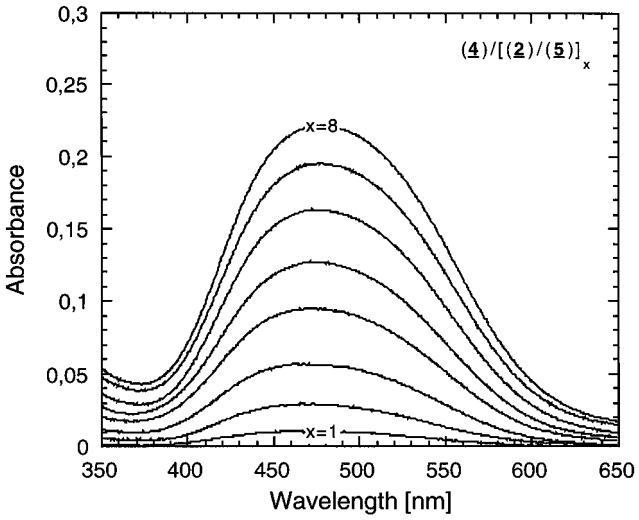

Figure 13. UV/vis spectra of coated PP after the deposition of successive **2**/**5** layer pairs on the primer polymer **4** layer.

polymer **2** remains higher for an assembly with copolymer **4** as cation than for an assembly with polymer **3** as cation (Figure 12). Also the slopes indicate the deposition of more material in the case of the **2**/**4** assembly: for this assembly, the slope is 0.019 per deposition cycle, while the **2**/**3** system exhibits a slope of 0.012 per deposition cycle only.

The regular deposition of a more complex hydrophobized, colored polymer, instead of the polycation in the multilayer, was also investigated (see Chart 1; polymer **5**). After a primer copolymer **4** layer, polymer **2** and **5** layers were alternated in order to obtain the assembly **4**/[**2**/**5**]$_x$. The colored polycation allows us to check the macroscopic quality of the coating by eye and on a smaller length scale by light microscope. Actually, the sample **4**/[**2**/**5**]$_4$ shows an homogeneous orange-red color due to the polymer **5** layers, indicating the good overall coverage of the poly(propylene) support. In Figure 13, the UV/vis spectra of multilayer assemblies from polymers **2** and **5** after different numbers of deposition cycles are shown. The first cycle after the deposition of polymer **4** results in a weak intensity, but then a linear increase is observed, indicating a regular and reproducible assembly.

The assembly **4**/[**2**/**5**]$_4$ was characterized by ToF-SIMS and XPS. The negative ToF-SIMS spectrum of this sample

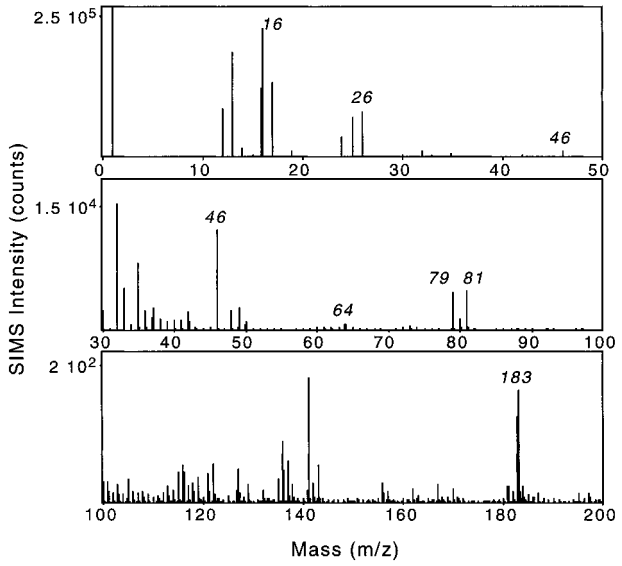

Figure 14. Negative ToF-SIMS spectrum of coated PP after deposition of the multilayer **4**/[**2**/**5**]$_4$.

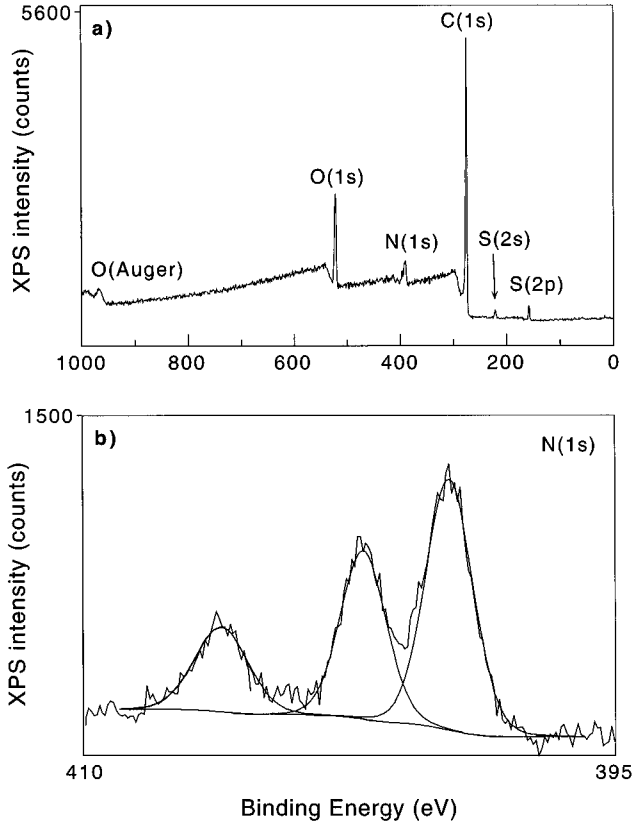

Figure 15. XPS spectra of the multilayer **4**/[**2**/**5**]$_4$: (a) general spectrum; (b) detailed spectrum of the N 1s line.

is displayed in Figure 14. The most characteristic feature of polymer **5** is the large NO_2^- peak (m/z = 46). Intense CN^- and S^- peaks are also present, showing the important amount of nitrogen and sulfur in the top layers. The Br^- counterion isotopes (m/z = 79 and 81) are present with particularly high intensities, indicating that a low but significant amount of these ions are trapped in the multilayer. At higher mass, the dominant peak is due to the repeat unit of polymer **2**, $C_8H_7SO_3^-$ (m/z = 183). Notwithstanding the complex structure of polymer **5**, the positive spectrum of the sample is rather uncharacteristic. The large fraction of heteroatoms leads to numerous bond scissions inside the monomer and to the production of

very small charged fragments. However, some large ions carrying the charged group of the polymer could be detected with significant intensities: $C_{10}H_9N_2^+$ (m/z = 157); $C_{11}H_{10}N_2^+$ (m/z = 170); $C_{12}H_{11}N_2^+$ (m/z = 183); $C_{13}H_{13}N_2^+$ (m/z = 197) and $C_{14}H_{15}N_2^+$ (m/z = 211).

The XPS spectra of the assembly **4**/[**2**/**5**]$_4$ confirm the deposition of polymer **5** (Figure 15). The large nitrogen and the lower sulfur percentages (Table 3) are consistent with the formula of the **2**/**5** pair. The three components of the N 1s peak (Figure 15b) can be attributed to (i) the nitrogen-containing aromatic and aliphatic groups (BE = 399.7), (ii) the charged groups (BE = 402.2 eV), and (iii) the NO_2 group (BE = 406.2 eV). The experimental ratio of the three components of N 1s is 51:32:17, which is very close to the chemical structure of polymer **5** (3:2:1).

4. Conclusion

The surface analysis techniques show that alternate polyelectrolyte thin films may be built up on polymer substrates. Within the series of polymer supports tested (poly(propylene), poly(isobutylene), poly(styrene), poly(methyl methacrylate), poly(ethylene terephthalate), poly(phenylene oxide), and poly(ether imide)), the best substrate coverage is obtained on polar semicrystalline PET for the assembly **1**/[**2**/**3**]$_3$. In general, the promising results obtained with polymer supports containing carbonyl groups and/or benzene rings suggest that these electron-rich functionalities develop rather specific interactions with the charged groups of the polycation. In contrast, the deposition of **1**/[**2**/**3**]$_3$ on the aliphatic hydrocarbons (PP and PIB) is problematic. This is probably due to the particularly weak interaction between the polyelectrolyte and these apolar polymers.

In the case of PET, the detailed analysis of the samples after each deposition cycle suggests that the amount of polycation **3** deposited increases with the layer number, which was not the case on silicon. In addition, the non-linear correlation between SIMS and XPS intensities shows that the attenuation of the substrate intensities is not due to a gradual filling of coating holes or defects but to a real increase of the whole sample thickness at each step.

The results obtained on poly(propylene) indicate that the successful multilayer buildup depends not only on the substrate−primer layer interaction but also on the nature of the following layers. The use of a copolymer containing long alkyl residues instead of the primer polymer **1** layer gives much better results only if the same copolymer is used instead of polycation **3** at the following deposition cycles too (assembly **4**/[**2**/**4**]$_3$): in that case, the characteristic signals of the coating in SIMS and XPS are higher, whereas those of the substrate are lower, and the increase of the UV absorbance with the layer number is more pronounced. Finally, the deposition of a colored, NLO polymer as polycation in the multilayer could be achieved on poly(propylene) as well.

Acknowledgment. The authors wish to thank R. Legras, A. Jonas, X. Arys, and B. Laguitton (U.C.L) for helpful discussions. This work was supported by the "Action de Recherche Concertée" (94/99-173) of the "Communauté Française de Belgique, Direction Générale de l'Enseignement Supérieur et de la Recherche Scientifique". The ToF-SIMS equipment was acquired with the support of the "Région Wallonne" and "FRFC-Loterie Nationale" of Belgium.

LA970105O